Heliyon 10 (2024) e34173

Contents lists available at ScienceDirect

Heliyon

journal homepage: www.cell.com/heliyon

Research article

Enhancing clinical safety in bioengineered-root regeneration: The use of animal component-free medium

Yuzhen Zhan [a,b,c,1], Aizhuo Qian [a,b,c,1], Jieya Gao [d], Shiyong Ma [d], Pingmeng Deng [a,b,c], Hefeng Yang [e], Xiaonan Zhang [a,b,c], Jie Li [a,b,c,*]

[a] College of Stomatology, Chongqing Medical University, Chongqing, China
[b] Chongqing Key Laboratory of Oral Diseases, Chongqing Medical University, Chongqing, China
[c] Chongqing Municipal Key Laboratory of Oral Biomedical Engineering of Higher Education, Chongqing Medical University, Chongqing, China
[d] Basic Medicine Research and Innovation Center for Novel Target and Therapeutic Intervention, The Ministry of Education, Institute of Life Sciences, Chongqing Medical University, Chongqing, China
[e] Yunnan Key Laboratory of Stomatology, The Affiliated Stomatology Hospital of Kunming Medical University, Kunming, China

ARTICLE INFO

Keywords:
Animal component-free medium
Bioengineered-root regeneration
Human-treated dentin matrix
Three-dimensional culture

ABSTRACT

Background: Most studies used animal serum-containing medium for bioengineered-root regeneration, but ethical and safety issues raised by animal serum are a potentially significant risk for clinical use. Thus, this study aimed to find a safer method for bioengineered-root regeneration.
Methods: The biological properties of human dental pulp stem cells (hDPSCs) cultured in animal component-free (ACF) medium or serum-containing medium (5%, 10% serum-containing medium, SCM) were compared *in vitro*. hDPSCs were cultured in a three-dimensional (3D) environment with human-treated dentin matrix (hTDM). The capacity for odontogenesis was compared using quantitative real-time PCR (qPCR) and Western blot. Subsequently, the hDPSCs/hTDM complexes were transplanted into nude mice subcutaneously. Histological staining was then used to verify the regeneration effect *in vivo*.
Results: ACF medium promoted the migration of hDPSCs, but slightly inhibited the proliferation of hDPSCs in the first three days of culture compared to SCM. However, it had no significant effect on cell aging and apoptosis. After 7 days of 3D culture in ACF medium with hTDM, qPCR showed that *DMP1, DSPP, OCN, RUNX2*, and *β-tubulin III* were highly expressed in hDPSCs. In addition, 3D cultured hDPSCs/hTDM complexes in ACF medium regenerated dentin, pulp, and periodontal ligament-like tissues similar to SCM groups *in vivo*.
Conclusion: ACF medium was proved to be an alternative medium for bioengineered-root regeneration. The strategy of using ACF medium to regenerate bioengineered-root can improve clinical safety for tooth tissue engineering.

1. Introduction

Tooth loss is one of the common oral diseases, often affecting pronunciation and chewing, thereby impacting the quality of life.

* Corresponding author. College of Stomatology, Chongqing Medical University. 426# Songshibei Road, Yubei District, Chongqing, 401147, China.
E-mail address: jieli@hospital.cqmu.edu.cn (J. Li).
[1] These authors contributed equally to this work.

https://doi.org/10.1016/j.heliyon.2024.e34173
Received 26 March 2024; Received in revised form 27 June 2024; Accepted 4 July 2024
Available online 5 July 2024

Clinically, fixed bridges, removable partial dentures, and implant restorations are usually used to replace lost teeth with artificial materials [1–3]. Although these therapies have been widely used in the restoration of tooth loss, these materials only address the functional and aesthetic aspects of teeth, and do not regenerate the anatomical and functional structures [4]. Currently, researchers are working to find a better regeneration method for reconstructing the tooth root [5,6]. The tooth root is made up of soft tissues (dental pulp, periodontal ligament) and hard structures (dentin, cementum), functioning to bear and disperse occlusal forces [7]. Bioengineered-root regeneration is seen as a feasible and promising way to restore a lost natural tooth root [8,9].

The field of bioengineered-root regeneration has made significant progress thanks to stem cell-based tissue engineering technology [10,11]. Researchers have designed bioengineered-root based on stem cells to mimic natural tooth root. Human-treated dentin matrix (hTDM), as an appropriate biological scaffold with a three-dimensional (3D) structure, has been used in tissue engineering for the regeneration of bioengineered-root [9,12]. hDPSCs have great potential in regenerative medicine, therefore, it can be used for therapy and bioengineered-root regeneration [13]. However, it has been reported that cells were cultured in animal component-containing medium for biological tissue engineering mostly at present [10,14].

Animal serum-containing medium may pose many risks [15]. Several research studies have demonstrated that the inclusion of animal-derived serum as an ingredient is controversial due to the potential risk of transmitting illnesses caused by proteins such as prions, viruses, mycoplasmas, zoonotic infections, or viral infections [16–18]. Animal serum may contain amounts of hemoglobin, endotoxin, and other harmful factors, which affect the safety of product [19]. Additionally, differences in the quality and protein concentration of serum from different batches affect the reproducibility of experiments [20]. Moreover, some research has demonstrated that human platelet lysate was an essential serum supplement for the clinical-grade growth of a variety of cells. However, its chemical composition is still unclear, and peripheral or umbilical cord blood cannot satisfy the requirements for large-scale stem cell proliferation [21]. Therefore, it is urgent to develop animal component-free medium for tissue engineering and future clinical translation.

To address the ethical concerns and safety risks associated with animal components, researchers have developed animal component-free (ACF) media for the cultivation of diverse mesenchymal stem cells from bone marrow [22], umbilical cord [23], adipose tissue [24], periodontal membrane [25], and dental pulp [26]. Studies have shown that hDPSCs can generate neurospheres in suspension under ACF culture conditions and differentiate into nerve cells, which may be used for clinical treatment of neurodegenerative diseases in the future [27,28]. Researchers demonstrated that the adherence ability, proliferation ability, and stem cell markers of hDPSCs cultured in ACF medium were improved [29,30]. The results suggest that ACF medium has clinical application value. Yet, it is still unclear whether ACF medium can be used for bioengineered-root regeneration.

This study is to evaluate the effect of ACF on bioengineered-root regeneration. Our work employed hTDM as scaffold material to assess the odontogenic potential of hDPSCs cultured in a 3D environment in either ACF medium or serum-containing medium (SCM). The results showed that hDPSCs cultured in ACF medium exhibit slightly different biological characteristics compared to those cultured in SCM. Besides, ACF culture in a 3D environment regenerated dentin, pulp, and periodontal ligament-like tissues similar to SCM *in vivo*. This study provides a new direction for addressing the safety and ethical issues in clinical applications.

2. Materials and methods

Ethical statement

The Helsinki Declaration's ethical criteria were followed in the establishment of the experimental protocol. And Chongqing Medical University College of Stomatology Ethics Committee authorized the experimental protocol (NO: 2022 (LSNo. 115)). Participants, either as individuals or as guardians, gave written informed consent.

2.1. Treatment of human dentin matrix

Premolars were extracted from individuals for therapeutic purposes at Stomatology Hospital of Chongqing Medical University. hTDM was prepared the same as the previous research [10,31,32]. In a nutshell, mechanical methods were mostly used to remove dental pulp tissues, pre-dentin, cementum, and a portion of dentin. After being demineralized through gradient EDTA (Sigma-Aldrich, St. Louis, MO, USA) for 20 min each, the human dentin matrix was washed with deionized water. Human-treated dentin matrices were kept in a Penicillin-Streptomycin solution (Hyclone, Logan, UT, USA) for 24 h. Subsequently, after being repeatedly rinsed in PBS, they were submerged in 70% alcohol for 10 min and finally stored at −80 °C. The surface morphology of hTDM was photographed via scanning electron microscopy (SEM, Hitachi TM4000PLUS II,Tokyo, Japan).

2.2. Isolation and culture of hDPSCs

Teeth were collected for cell isolation and culture from healthy young patients between the ages of 16–22 who had impacted third molars and orthodontic teeth that needed to be extracted for orthodontic therapy. Dental pulp was washed with phosphate-buffered saline (PBS, Solarbio, Beijing, China). After chopping the tissues into tiny pieces, they were digested for 0.5 h at 37 °C via 3 mg/mL type I collagenase (Sigma-Aldrich, St. Louis, MO, USA). Following this, the tissues were incubated in α-minimum essential medium (α-MEM, Hyclone, Logan, MO, USA) supplemented with 10% fetal bovine serum (FBS, Gemini Bio-Products, Woodland, CA, USA) at the temperature of 37 °C in air that is humidified and contains 5% carbon dioxide. After hDPSCs reached a concentration of 80%, they were trypsinized and passaged. Cells were cultured in different conditions at Passage 2 (P2): in the animal component-free medium

(MesenCult™-ACF Plus Medium, ACF, Stemcell Technologies, Vancouver, BC, Canada) and serum-containing medium (5%, 10% serum-containing medium, SCM). Cell suspensions were cultured in ACF medium with the density of 1×10^5 cells/mL, then passaged at least twice for the following analysis. Observing and comparing the morphological changes at 24 h and 48 h after hDPSCs seeding into the three media by the phase-contrast inversion microscope (Olympus, Tokyo, Japan).

2.3. Flow cytometric characteristic analysis

hDPSCs were trypsinized into single-cell suspensions and centrifuged for 5 min to assess cell surface markers' expression. About 5×10^5 cells were incubated for 30 min for flow cytometric analysis at room temperature using Fluorescein Isothiocyanate (FITC)-conjugated antibodies against CD14, CD45, CD90, CD146, and isotype control, respectively. All the antibodies were obtained from BD Biosciences, a division of Becton-Dickinson (CA, USA). FACS Caliber (BD, CA, USA) was applied for the flow cytometry analysis. At least three repetitions of the experiment were conducted.

2.4. Immunofluorescence

hDPSCs (1×10^5 cells/mL) were plated on the cell climbing pieces in 12-well plate. Washing cells twice with PBS (Solarbio, Beijing, China). After being fixed for 15 min using 4% paraformaldehyde (Beyotime, Shanghai, China), rinse three times for 10 min each time. It was cleaned three times with PBS for a total of 10 min after being treated for 5 min using 0.1% Triton X-100 (Sigma-Aldrich, St. Louis, MO, USA) as the penetrator. hDPSCs were covered with 300 μL 1 × iFluro™ 555 phalloidin (Yeasen Biotechnology, Shanghai, China) and stained for 90 min in the dark, followed by two 5-min washes with PBS. The nuclei were stained for 5 min with DAPI (Beyotime, Shanghai, China), followed by two 5-min washes with PBS. Using a fluorescence microscope (Thermo Scientific, USA) to observe hDPSCs. The experiment was conducted at least three times.

2.5. Colony formation assay

hDPSCs (1×10^3 cells/mL) were placed at 37 °C in the 10 cm plate with 5% CO_2-saturated humidity and incubated for 10 days. The culture was terminated when macroscopic clones appeared in plates. Discard the supernatant and carefully wash three times using PBS. After being fixed for 15 min using 4% paraformaldehyde (Beyotime, Shanghai, China), cells were stained for 20 min using crystal violet (Beyotime, Shanghai, China). At least three repetitions of the experiment were conducted.

2.6. Cell proliferation

The quantitative assessment of hDPSCs' activity was conducted via the Cell Counting Kit-8 (CCK-8, Dojindo, Kumamoto, Japan). After being digested, hDPSCs (1×10^3 cells/well) were placed in 96-well plates. The original medium was replaced with 1:9 CCK-8 solution and culture medium. The microplate reader was applied to measure the absorbance at a wavelength of 450 nm after incubating for 4 h at 37 °C. After 0, 1, 3, 5, and 7 days of incubation, the test was performed according to the directions for the Cell Counting Kit. The average data was used to plot the CCK-8 growth curves. At least three repetitions of the experiment were conducted.

2.7. SA-β-gal staining

hDPSCs were harvested at passage 10 and rinsed 3 times with PBS before being immobilized for 15 min in 4% paraformaldehyde solution. The cells were stained via the SA-β-gal staining kit (Beyotime, Shanghai, China) for an overnight period of time at 37 °C. The quantity of blue cells (SA-β-gal positive cells) was observed under the microscope. At least three repetitions of the experiment were conducted.

2.8. Analysis of the cell cycle

Trypsin digested hDPSCs into single cells, which were subsequently centrifuged in PBS buffer at $300 \times g$ for 5 min. The liquid portion was removed, and the process was done twice. After resuspending 1×10^6 cells in 0.1 mL of PBS buffer with the Cell Cycle Kit (Beyotime, Shanghai, China), gradually add 500 μL of precooled 75% ethanol. Data were obtained from CytoFLEX (Beckman Coulter, Inc., Brea, California, USA). At least three repetitions of the experiment were conducted.

2.9. Cell apoptosis analysis

The hDPSCs were digested with trypsin and then centrifuged in PBS buffer at $300 \times g$ for 5 min. The liquid portion was removed, and the process was done twice. Finally, 500 μL of PBS solution were used to resuspend 1×10^6 cells, and propidium iodide (PI) staining was performed. CytoFLEX (Beckman Coulter, Inc., Brea, CA, USA) was applied to capture the data, and FlowJo software was employed to determine the proportion of cells at different periods on the PI fluorescence histogram. At least three repetitions of the experiment were conducted.

2.10. Cell migration ability analysis

Use a marker pen to draw straight lines at a spatial separation of 1 cm on the back of the six-well plate. hDPSCs (1×10^5 cells/mL) were placed onto 6-well plates and cultured under various conditions. After cells reached a concentration of 80%, scratch cells according to the marked line with the tip of a pipette. Samples were tested at 0 h, 12 h, and 24 h, respectively. At least three repetitions of the experiment were conducted.

2.11. Osteogenic differentiation

2×10^5 hDPSCs were planted in the 6-well plate after passing various growth conditions. After 80% confluency was obtained, cells were cultured in osteogenic media comprising 10% FBS, 50 μg/mL ascorbic acid (Sigma-Aldrich, St. Louis, MO, USA), 100 μM dexamethasone (Sigma-Aldrich, St. Louis, MO, USA), and 10 mM L-glycerophosphate (Sigma-Aldrich, St. Louis, MO, USA) for 7 and 21 days. Every two or three days, the media were refreshed. They were immobilized with 4% paraformaldehyde solution for 15 min after 7 and 21 days. After being PBS-washed twice, 30 min of room-temperature incubation with the Alkaline Phosphatase Staining Kit (Beyotime, Shanghai, China) and 1% Alizarin Red solution (Sigma-Aldrich, St. Louis, MO, USA) were conducted. After the samples were thoroughly cleansed with purified water, they were photographed via a phase-contrast inverted microscope (Olympus, Tokyo, Japan). The calcium content of the calcified nodules was ascertained by assessing the absorbance at 560 nm via a microplate reader (PerkinElmer, Waltham, Massachusetts, USA) following the elution of the nodules with 10 mM sodium phosphate containing 10% cetylpyridinium chloride hydrate (Sigma-Aldrich, St. Louis, MO, USA). At least three repetitions of the experiment were conducted.

2.12. 3D culture of hDPSCs

5×10^5 and 2×10^5 hDPSCs were seeded in the 3D culture system constructed with hTDM scaffolds and low adhesion 6-well culture plates (Sumiron, Osaka, Japan). Morphological observations were made via the phase-contrast inversion microscope (Olympus, Tokyo, Japan) at 0, 12, and 24 h. F-actin staining was conducted after hDPSCs/hTDM complexes formation. The method is as described above. Furthermore, a laser confocal microscope (Leica Optical, Wetzlar, Germany) was applied to observe hDPSCs/hTDM complexes. At least three repetitions of the experiment were conducted.

2.13. Morphometric analysis

The acquired images and data will be processed and analyzed using the customized code written by Python 3.8 to make full use of its image visualization and processing capabilities. The circularity of a cell is represented by the circularity index ($CI = 4\pi A/L^2$), where A is the cell's area, L is its circumference, and $CI = 1$ denotes a complete circle. The aspect ratio (AR), which depicts the symmetry of a cell, is determined as the ratio of the longest axis to the shortest axis of the cell [33]. In a previous work [34], radial mean intensity (RMI) was used to measure protein distribution without considering cell shape. RMI calculates a protein's average intensity as a function of its distance from the cell's center and edge.

Table 1
Oligonucleotide primer sequences.

Target cDNA	Primer sequence(5'–3')	Product length	Accession No.
DSPP	F TTTGGGCAGTAGCATGGGC R CCATCTTGGGTATTCTCTTGCCT	199	NM_014208.3
DMP1	F CACTCAAGATTCAGGTGGCAG R TCTGAGATGCGAGACTTCCTAAA	75	NM_001079911.3
POSTN	F CTCATAGTCGTATCAGGGGTCG R ACACAGTCGTTTTCTGTCCAC	138	NM_001135935.2
OCN	F CTCACACTCCTCGCCCTATTG R CTCCCAGCCATTGATACAGGTAG	166	NM_199173.6
COL-1	F GAGGGCCAAGACGAAGACATC R CAGATCACGTCATCGCACAAC	140	NM_000088.4
RUNX2	F CTTTACTTACACCCCGCCAGTC R AGAGATATGGAGTGCTGCTGGTC	146	NM_001015051.4
TGF-β1	F ATTTATTGAGCACCTTGGGCAC R TCTCTGGGCTTGTTTCCTCAC	130	NM_000660.7
ALP	F TAAGGACATCGCCTACCAGCTC R TCTTCCAGGTGTCAACGAGGT	170	NM_001127501.4
β-tubulinIII	F AGATCGGGGCCAAGTTCTG R CGAGGCACGTACTTGTGAGA	142	NM_006086.4
GAPDH	F CTTTGGTATCGTGGAAGGACTC R GTAGAGGCAGGGATGATGTTCT	132	NM_001357943.2

2.14. Scanning electron microscope (SEM)

After co-culturing hDPSCs with hTDM for 4 days, the samples were cleaned and fixed using a unique fixative (Beyotime, Shanghai, China) for an electron microscope. The samples were sprayed with a layer of gold and examined using the scanning electron microscope (SEM, TM4000PLUS II, Hitachi, Tokyo, Japan) after being dehydrated with ethanol. At least three repetitions of the experiment were conducted.

2.15. Quantitative real-time PCR

Our study employed qPCR to detect and compare the expression of odontogenic differentiation-related genes (*DSPP, OCN, ALP,*

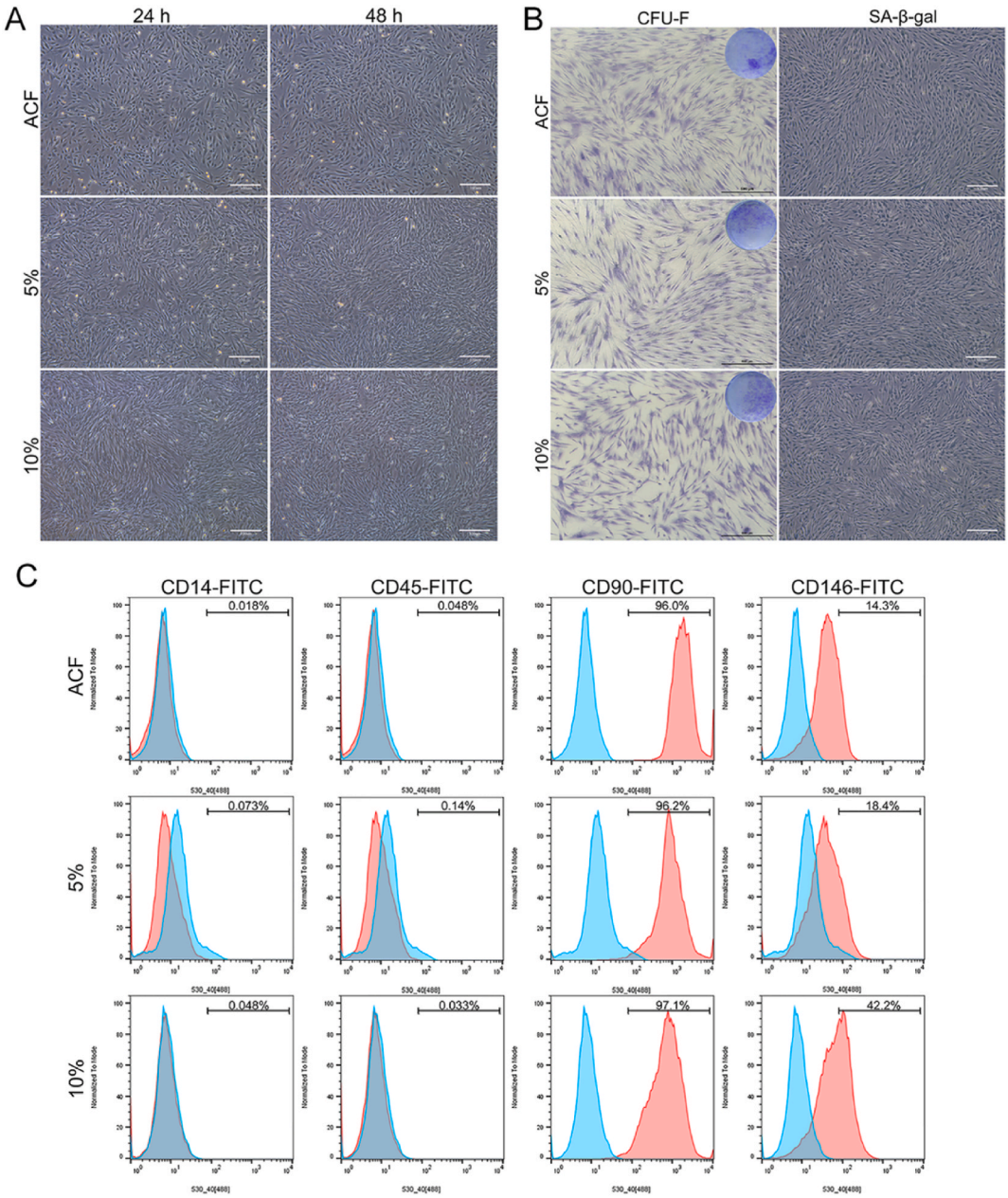

Fig. 1. Cell morphology and identification of human dental pulp stem cells. (A) Cell morphology after cultured in ACF medium and SCM for 24 h and 48 h. Scale bars = 100 μm. (B) Crystal violet staining of colony forming unit fibroblasts of the three groups. ACF, 5 %, 10 %, scale bars = 500 μm. β-Galactosidase staining of hDPSCs cultured in the three media. Scale bars = 100 μm. (C) Flow cytometric characteristic analysis of hDPSCs cultured in the three media.

DMP-1, β-Tubulin III, COL-1, POSTN, RUNX2, and TGF-β1). hDPSCs were cultured with hTDM. hDPSCs/hTDM in ACF medium was the experimental group, hDPSCs/hTDM in 5% and 10% serum-containing medium were the control groups. Following the manufacturer's directions, the RNAiso Plus reagent was applied to obtain the whole RNA. The expression of *DSPP, DMP-1, COL-1, OCN, ALP, POSTN, RUNX2, β-Tubulin III, TGF-β1,* and *GAPDH* were all assessed. The $2^{-\Delta\Delta CT}$ approach was employed to compute relative levels, which were standardised against the reference GAPDH gene. The primer sequences for this calculation are provided in Table 1. Three repetitions of the experiment were conducted.

2.16. Western blot

The Total Protein Extraction Kit (Beyotime, Shanghai, China) was applied to digest hDPSCs, and then they were sonicated for 30 min. The protein concentration was determined through the utilization of BCA analysis. Proteins were separated on polyacrylamide gel with 10% sodium dodecyl sulfate, transferred to a membrane made of polyvinylidene fluoride (PVDF), then covered with 5% non-fat milk diluted in TBST (Tris-buffered saline, 0.1% Tween-20). The primary antibodies anti-Integrin αV (ABclonal Technology, Wuhan, China), anti-FAK (ABclonal Technology, Wuhan, China), anti-pFAK (ABclonal Technology, Wuhan, China), anti-DMP1 (Santa Cruz Biotechnology, CA, USA), anti-TGF-β1 (Santa Cruz Biotechnology, CA, USA), and anti-RUNX2 (Cell Signaling Technology, MA, USA) were deliquate at 1:1000 and incubated at a temperature of 4 °C overnight with the sample. Subsequently, the samples underwent three washes with TBST, every time for 10 min. The secondary antibodies against rabbits or mice derived from goats were diluted at 1:3000 in 1% non-fat milk dissolved in TBST, and then left to incubate with the sample for 1 h. The membranes had three TBST washes. The strips were monitored using an electrochemiluminescence system (Bio-Rad, CA, USA). At least three repetitions of the experiment were conducted.

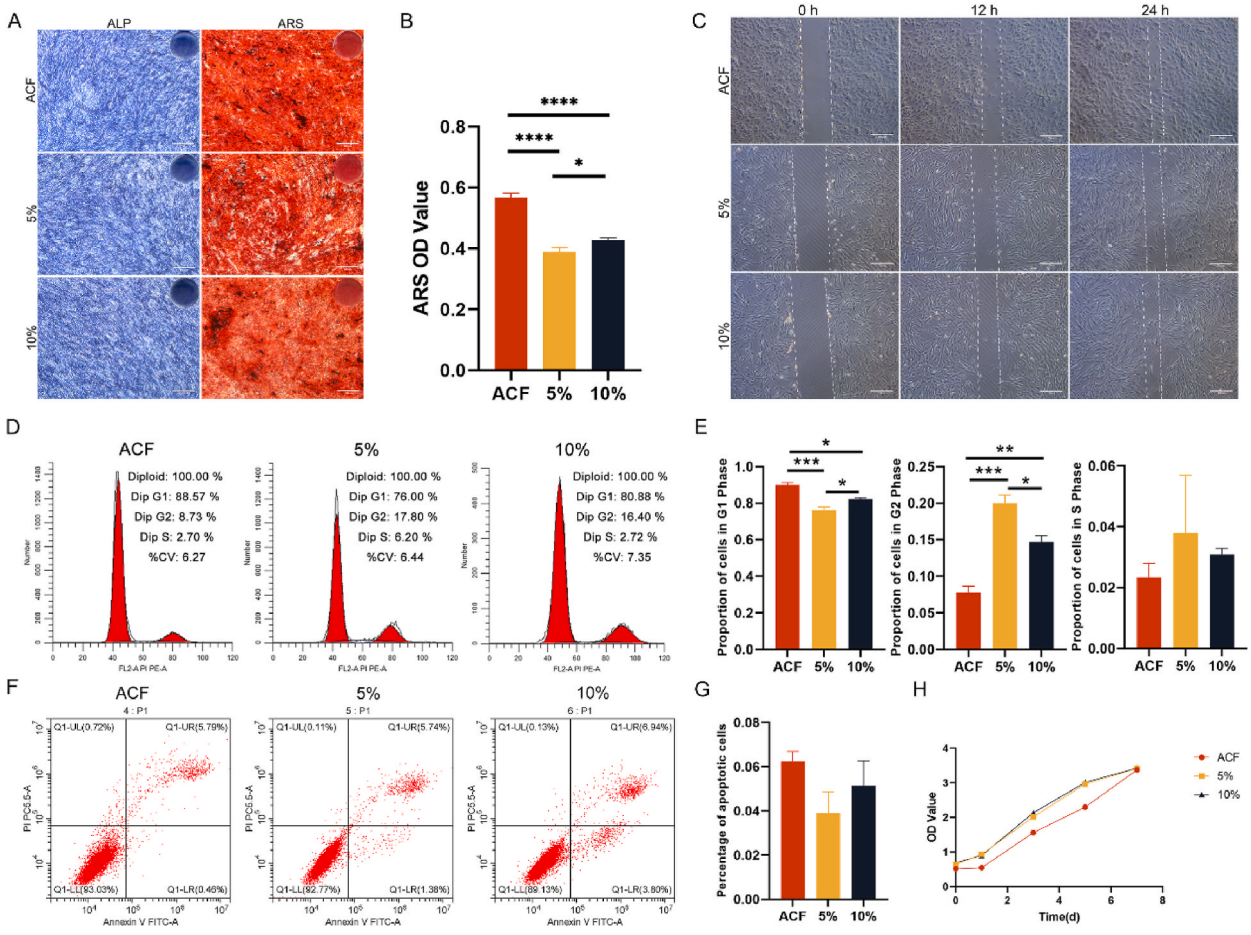

Fig. 2. Biological characteristics of hDPSCs cultured in the three media. (A) ALP staining results of the three groups after 7 days of osteogenesis induction. Alizarin red staining results of the three groups after 21 days of osteogenesis induction. (B) Statistical analysis of alizarin red staining showed differences among the three groups. (C) Scratch test of hDPSCs cultured in the three media. (D) Cell cycle of hDPSCs cultured in the three media. (E) Quantitative analysis of cell proportion of the three groups. (F) Apoptosis rate of the three groups. (G) There is no significant difference in apoptosis rate among the three groups. (H) CCK-8 results of hDPSCs proliferation rate of the three groups. Scale bars = 100 μm *p < 0.05, **p < 0.01, ***p < 0.001, ****p < 0.0001.

2.17. Evaluation of the in vivo regenerative capacity of hDPSCs/hTDM complex

The nude mice were bought from TengXin Biotechnology Co., Ltd (Chongqing, China). hDPSCs/hTDM complexes were implanted into immunodeficient mice's dorsal side (8-week-old male, n = 6) under general anesthesia with isoflurane. Three groups of nine immunodeficient mice were created randomly: (1) hDPSCs/hTDM complexes cultured in ACF; (2) hDPSCs/hTDM complexes cultured in 5% SCM; and (3) hDPSCs/hTDM complexes cultured in 10% SCM. Two samples were implanted in each mouse. Following an 8-week period, all samples from immunodeficient mice were collected. Following a 48-h fixation with a 4% paraformaldehyde solution, the samples were demineralized with 17% EDTA for 6 months, subsequently, dehydrated and embedded in paraffin. For Masson's trichrome, H&E, and immunohistochemical staining, paraffin slices were produced. The expression of POSTN, DSPP, DMP1, CAP, and TGF-β1 was determined by immunohistochemistry.

2.18. Statistical analysis

For statistical analysis, one-way ANOVA was performed. The outcomes are expressed using the mean and standard error of the mean (SEM). GraphPad Prism 9.0.0 was applied to conduct statistical analysis. The statistical significance observed was $P < 0.05$.

3. Results

3.1. Characteristics of stem cells identified in various media

The morphology of hDPSCs cultured in ACF medium was slightly different from that in SCM under an inverted microscope. Cells cultured in SCM were typical long spindle shape, while cells cultured in ACF medium were short spindle shape (Fig. 1A). No senescent cells were visible at P10, according to the results of cell senescence experiment (Fig. 1B). Crystal violet staining results revealed that cells cultured in all three groups formed colonies from a single cell (Fig. 1B). The results of flow cytometric analysis showed that CD14

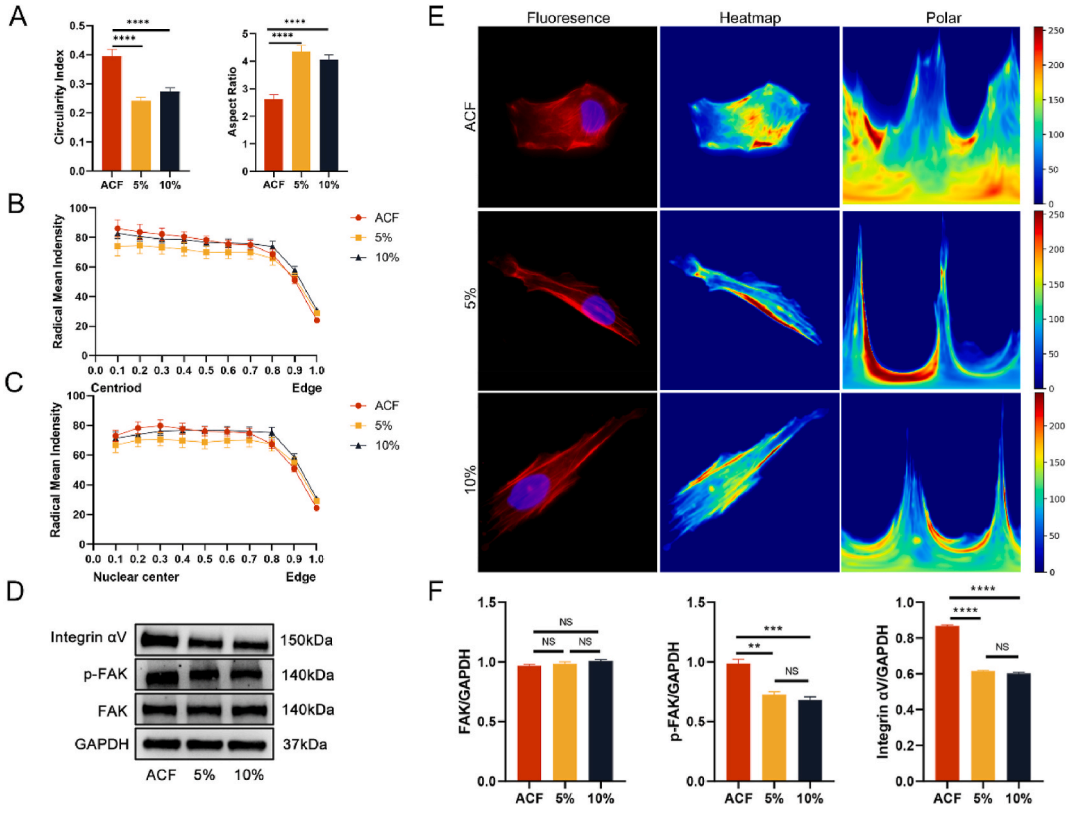

Fig. 3. Morphometric analysis results and Western blot. (A) The circularity index (CI) and aspect ratio (AR) of a single hDPSC cultured in the three media. (B) Radial Mean Intensity (RMI) is the distance between the cell centroid and the nearest edge and quantified the mean along all directions. (C) Radial Mean Intensity (RMI) is the distance between the nuclear center and the nearest edge and quantified the mean along all directions. (D) Western blot of Integrin αV, pFAK, FAK and GAPDH set as control. These original images of Western blot are presented in Data S1. (E) F-actin staining and heatmap and polar of actin intensity results of hDPSCs cultured in the three media. (F) The semi quantitative results of Integrin αV, FAK, pFAK. *$p < 0.05$, **$p < 0.01$, ***$p < 0.001$, ****$p < 0.0001$.

and CD45 were negatively expressed in cells cultured in the three media, while CD90 and CD146 were positively expressed, which were consistent with the surface markers expressed by mesenchymal stem cells. (Fig. 1C). This proves that the cells used in the experiment are dental pulp stem cells.

3.2. Biological characteristics of hDPSCs in different media

There was almost no difference among the three groups according to ALP staining. Alizarin red staining revealed that hDPSCs formed a lot of mineralized nodules in all three groups (Fig. 2A). According to quantitative results, ACF group exhibited the highest osteogenic ability, and it was statistically significant (Fig. 2B). In scratch test, the scratch width of the three groups was the same at beginning. After 12 h of incubation in ACF medium, obvious narrowing of the scratches was observed. After incubation for 24 h, the intercellular space disappeared in ACF group and nearly closed in the other two groups (Fig. 2C). This suggested that ACF medium can promote hDPSCs migration. According to cell cycle analysis, the percentage of hDPSCs during the G1 phase was 89.93% ± 1.35% in the ACF group, 76.21% ± 1.70% in 5% SCM group, and 82.20% ± 0.73% in 10% SCM group. In the G2 phase, the proportion of hDPSCs was 7.73% ± 0.90% in the ACF group, 20.01% ± 1.12% in 5% SCM group, and 14.71% ± 0.87% in 10 % SCM group. The fraction of hDPSCs in the S phase was 2.33% ± 0.46%, 3.78% ± 1.92%, and 3.09% ± 0.21% respectively (Fig. 2D and E). Annexin V and PI double staining showed that the three groups had apoptosis rates of 5.79% ± 1.35%, 3.92% ± 1.72%, and 5.43% ± 2.37%, respectively (Fig. 2F and G). The CCK-8 data revealed that in the first three days, the cell proliferation rate in the ACF group was slightly lower than that in the SCM groups. However, by the seventh day, it might be comparable to that in the SCM groups (Fig. 2H).

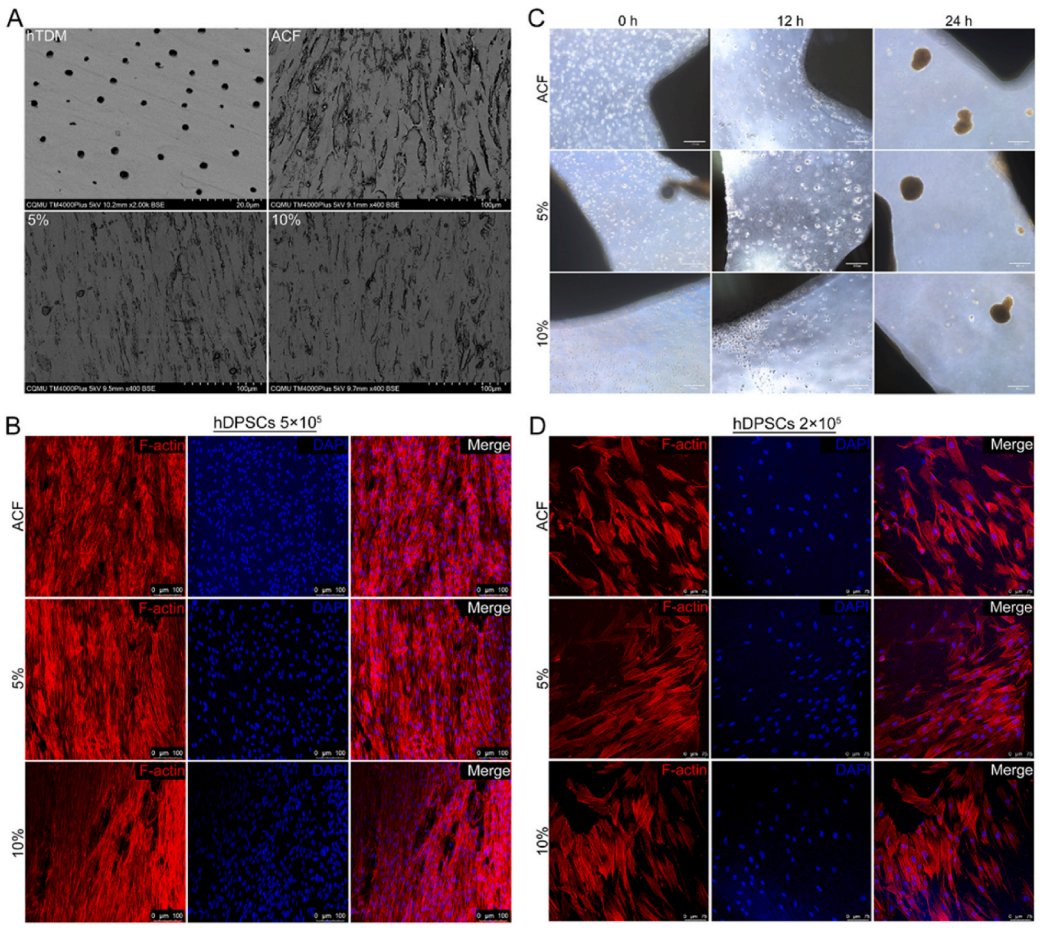

Fig. 4. hDPSCs/hTDM complexes cultured in three-dimensional condition. (A) SEM analysis result of hTDM before being co-cultured with hDPSCs, and the results of hDPSCs/hTDM complexes cultured in the three groups. Scale bar = 20 μm, scale bar = 100 μm. (B) F-actin staining results of 5×10^5 hDPSCs combined with hTDM cultured in the three media. Scale bar = 100 μm. (C) Changes of hDPSCs cultured from 0 h to 24 h around hDPSCs/hTDM complexes. Scale bar = 100 μm. (D) F-actin staining results of 2×10^5 hDPSCs combined with hTDM cultured in three media. Scale bar = 75 μm.

3.3. The morphology of hDPSCs cultured in ACF was different from that in SCM

We quantified cell morphology by measuring CI and AR. The findings revealed that CI value of ACF group was much higher than that of SCM groups. Nevertheless, there was no discernible difference between the groups with 5% and 10% FBS. In contrast, AR values

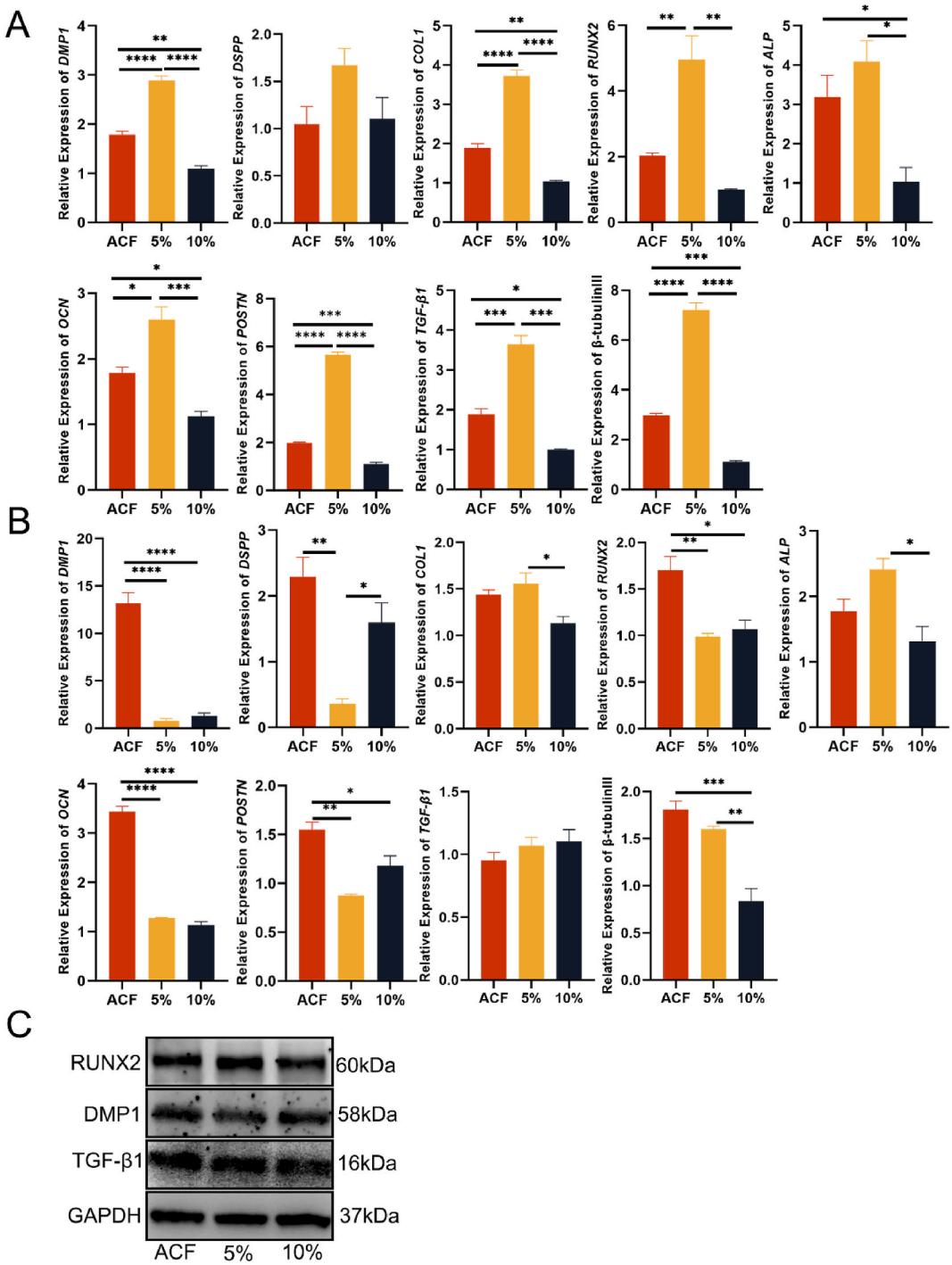

Fig. 5. Expression levels of odontogenesis-related genes and proteins in hDPSCs/hTDM complexes. (A) qPCR results of hDPSCs/hTDM complexes cultured in the three media after 4 days. (B) qPCR results of hDPSCs/hTDM complexes cultured in the three media after 7 days. (C) Western blot of RUNX2, DMP1, TGF-β1 and GAPDH set as control. There is no significant difference among the three groups. $^{*}p < 0.05$, $^{**}p < 0.01$, $^{***}p < 0.001$, $^{****}p < 0.0001$. These original images of Western blot are presented in Data S1.

of SCM groups were significantly greater than that of ACF group (Fig. 3A). The results of AR and CI showed that morphology of cells cultured in ACF was different from those cultured in SCM. We performed Radical Mean Intensity (RMI) analysis to better understand the cytoskeleton structure differences between the three groups of cells. The RMI data demonstrated that the ACF group's expression of RMI in the near cell center was higher than that of SCM groups, but it was lower in the far cell than that of SCM groups, among which 5% group was lowest overall (Fig. 3B and C). Western blot results showed that expression of Integrin αV and *p*-FAK was higher in the cells cultured in ACF medium than in SCM, while Integrin αV expression was comparable in the cells cultured in 5% and 10% groups. There was no discernible change in the expression of FAK among the cells cultured in the three media (Fig. 3D). The fluorescence, heatmap and polar results were consistent with the RMI (Fig. 3E). Semi-quantitative Western blot results showed that Integrin αV and *p*-FAK expression were significantly higher in hDPSCs cultured in ACF medium than in SCM (Fig. 3F).

3.4. Odontogenic differentiation comparison in vitro

The SEM revealed that the dentinal tubules of hTDM were completely exposed before being co-cultured with hDPSCs. After being co-cultured with hDPSCs for 4 days, the surface of hTDM exhibited high-density cells (Fig. 4A). Immunofluorescence analysis showed that most hDPSCs attached to the surface of hTDM in all three groups (Fig. 4B and D). The findings revealed that most cells stuck to the surface of hTDM, with only a minority of spherically shaped cells remaining suspended (Fig. 4C). These findings demonstrated that in 3D culture environment, hDPSCs adhered to the surface of hTDM. Additionally, mRNA expression was assessed by qPCR analysis after hDPSCs and hTDM were co-cultured in a 3D culture environment for 4 and 7 days. Results of hDPSCs/hTDM complexes cultured in the three media for 4 days revealed that the expression levels of *DMP1*, *DSPP, COL-1, RUNX2, ALP, OCN, POSTN, TGF-β1*, and *β-tubulin III* in the 5% group were highest, followed by the ACF group, with the lowest expression observed in the 10% group (Fig. 5A). However, after 7 days, the expression levels of *DMP1*, *DSPP, RUNX2, OCN, POSTN,* and *β-tubulin III* were highest in the ACF group. (Fig. 5B). The expression levels of RUNX2, DMP1, and TGF-β1 proteins were comparable among the three groups (Fig. 5C).

3.5. Bioengineered-root regeneration induced by hDPSCs in combination with hTDM cultured in ACF medium

After 8 weeks of subcutaneous implantation, all the samples were taken from nude mice. New pulp-like and dentin-like structures were generated inside of the hDPSCs/hTDM complexes of all groups. Besides, blood vessels were newly regenerated in the hDPSCs/hTDM complexes of all groups (Fig. 6A). Additionally, dentin-like tissues were formed outside of hDPSCs/hTDM complexes, and periodontal fibrous-like structures were generated outside the newly formed dentin-like structures in all three groups (Fig. 6B). Immunohistochemical analysis showed that the hDPSCs/hTDM complexes in all three groups produced dentin-specific proteins, DSPP and DMP-1, both within and outside of the complexes (Fig. 7). Besides, TGF-β1 was expressed in all three groups within and outside of the complexes, which indicated the regeneration of periodontal fibrous tissues and fibers in dental pulp (Fig. 8A). Additionally, all three groups expressed cementum-specific protein CAP, and periodontal fibrous connective tissue marker POSTN outside of hDPSCs/hTDM complexes (Fig. 8B). The thickness of freshly formed dentin and the expression of DMP1, DSPP, and TGF-β1 inside of the

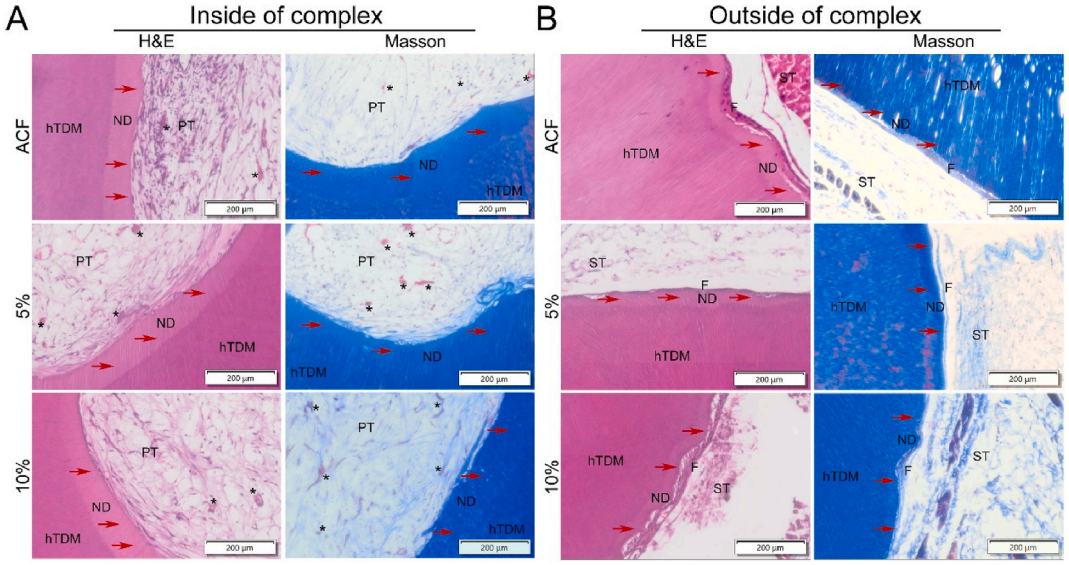

Fig. 6. H&E staining and Masson's Trichrome staining results inside and outside of the hDPSCs/hTDM complexes. (A) New pulp-like and dentin-like structures were formed inside of the hDPSCs/hTDM complexes *in vivo* after culturing in the three media. hTDM: human treated dentin matrix, ND: new dentin, red arrows indicate newly formed dentin, PT: pulp tissue, *: blood vessel. Scale bars = 200 μm. (B) Dentin-like and periodontal fibrous-like structures were formed outside the hDPSC/hTDM complexes *in vivo* after culturing in the three media. hTDM: human treated dentin matrix, ND: new dentin, red arrows indicate newly formed dentin, F: fibrous tissue, ST: skin tissue. Scale bars = 200 μm.

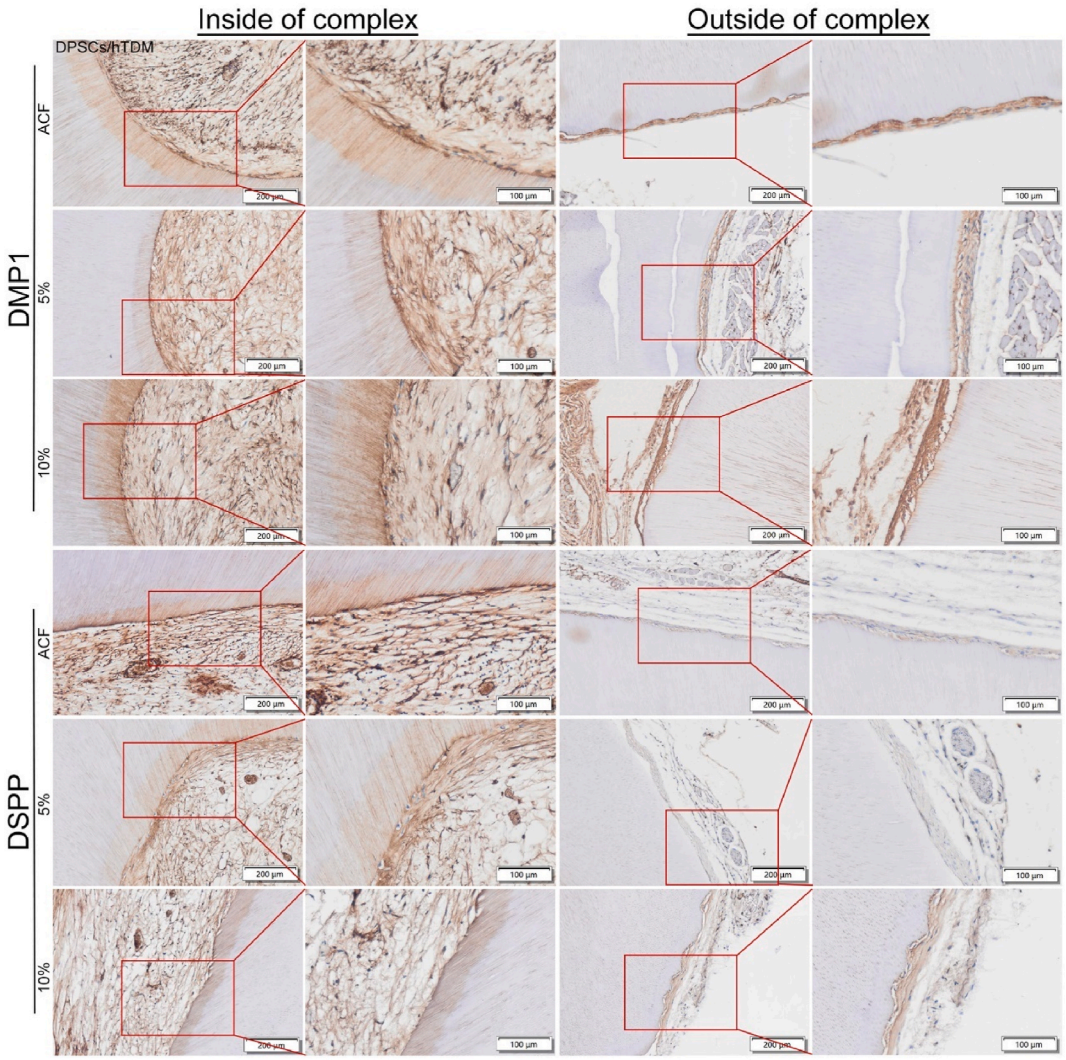

Fig. 7. Immunohistochemical evaluation of dentin regeneration inside and outside of the hDPSCs/hTDM complexes. DMP1 and DSPP expression were indicated by positive staining inside and outside of the hDPSCs/hTDM complexes *in vivo* after culturing in the three media. Scale bars = 200 μm in the first and third columns; scale bars = 100 μm in the second and fourth columns.

hDPSCs/hTDM complexes did not significantly differ among the three groups (Fig. 9).

4. Discussion

In the past decades, researchers have devoted themselves to transitioning human mesenchymal stem cells from basic research to clinical application. Several studies have focused on enhancing the circumstances for cell culture [35–37]. Considering the ethical and safety issues brought about by animal components, one of the most important achievements in this field will be the transition from animal component-containing medium to more clearly defined animal component-free medium. In addition, the animal component-free medium we employed for the experiment had previously been used to cultivate various types of stem cells [38–42]. Research has demonstrated that stem cells can be used for odontogenic differentiation to form bioengineered-root [43]. Dental stem cells have been applied to the regeneration of tooth-related tissues [10,12,44–47]. As far as we know, bioengineered-root regeneration in animal component-free medium has never been reported. In our experiment, we cultured the hDPSCs/hTDM complexes in the ACF medium and evaluated the capacity of odontogenesis and regeneration both *in vitro* and *in vivo*.

The findings of this research, which were consistent with those of previous studies, showed no discernible variation in the expression of immunophenotypic markers of mesenchymal stem cells in the three groups [10,14,48]. This suggests that the hDPSCs retrieved in this study satisfied the criteria of mesenchymal stem cells. Compared to SCM, cultured in ACF medium promoted the migration of hDPSCs. Additionally, it showed no substantial influence on cell aging or apoptosis. Although it slightly and briefly inhibited the proliferation of hDPSCs, ACF medium is overall suitable for the cell culture of hDPSCs.

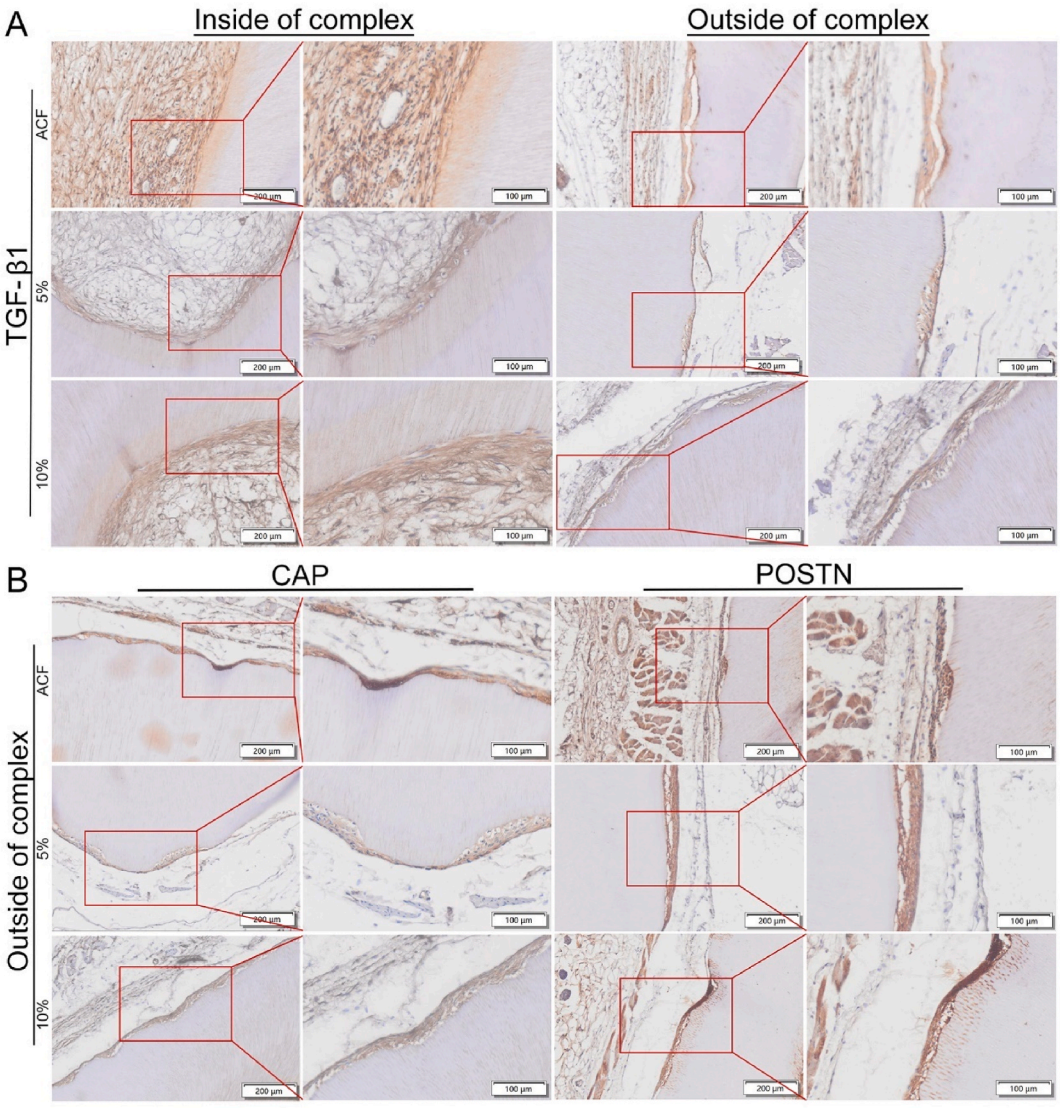

Fig. 8. Immunohistochemical evaluation of pulp, cementum, and periodontal fiber regeneration of the hDPSCs/hTDM complexes. (A) The expression of TGF-β1 was indicated by positive staining inside and outside of the hDPSCs/hTDM complexes *in vivo* after culturing in the three media. Scale bars = 200 μm in the first and third columns; scale bars = 100 μm in the second and fourth columns. (B) The expression of CAP and POSTN were indicated by positive staining outside of the hDPSCs/hTDM complexes *in vivo* after culturing in the three media. Scale bars = 200 μm in the first and third columns; scale bars = 100 μm in the second and fourth columns.

Previous studies [49,50] have shown that cell morphology affects the differentiation of mesenchymal stem cells. This study showed that the CI and AR values of hDPSCs cultured in ACF medium were closer to osteogenic/odontogenic differentiation value, which indicated that ACF medium may be suitable for culturing hDPSCs. Besides, earlier research [51] has demonstrated that integrin allows cells to regulate their morphology in response to signals from the extracellular matrix microenvironment. Therefore, we speculated that the components in ACF medium may change the cell morphology by modulating integrin αV and then activating FAK in the culture microenvironment. Additionally, the ACF group had a higher cell proportion in G1 phase than SCM, and the cell volume gradually increased in G1 phase [52]. This may be another reason why the cell morphology of ACF group looked slightly different from SCM groups. To figure out the specific mechanisms underlying morphological differences, more research is required.

Previous studies used odontogenic induction media to detect odontogenic ability *in vitro* [53]. In our experiment, we evaluated the odontogenic differentiation of *in vitro* hDPSCs/hTDM complexes. Due to the bioactivity advantages of hTDM, there was no need to use an odontogenic induction medium. DMP-1 is a specific protein in dentin [54]. A key component in the process of dentin production is the maturation of odontoblast cells, which exhibit the terminal phenotypic marker known as DSPP [55]. ALP, COL1, and OCN are crucial for the formation of minerals in dentin. Additionally, TGF-β1 not only serves as a marker for fibrous connective tissue, but also has various cytological functions, including regulating cell movement, growth, proliferation, differentiation, and apoptosis [56].

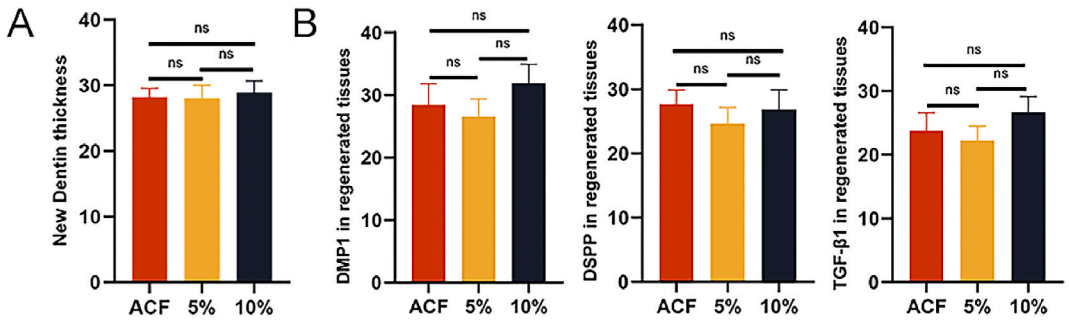

Fig. 9. Quantitative analysis of the new dentin thickness and the expression of odontogenesis-related genes. (A) Quantitative analysis results of H&E staining for new dentin thickness inside of the hDPSCs/hTDM complexes after culturing in the three media. There is no significant difference among the three groups. (B) Quantitative analysis results of immunohistochemical staining of DMP1, DSPP, and TGF-β1 expressions inside of the hDPSCs/hTDM complexes after culturing in the three media.

POSTN is especially expressed in connective tissues such as the periodontal ligament, and it participates in the reconstruction of periodontal tissues [57]. β-Tubulin III is a neuronal marker that can be used as an indicator to determine whether neural cell regeneration is present in the dental pulp [58]. The expressions of β-Tubulin III and TGF-β1 demonstrated the regeneration of fibers and nerves in the dental pulp. Upregulation of odontogenic/osteogenic markers indicated that ACF medium is suitable for bioengineered-root regeneration. Compared with the traditional cell culture medium containing 10% FBS, the medium with 5% FBS showed some differences in the expression of odontogenic/osteogenic markers. This suggested that the concentration of components in fetal bovine serum might be a significant factor influencing odontogenic differentiation. Previous studies using low serum and serum-free medium for cell culture have shown that low fetal bovine serum contains fewer risk components and requires less time, labor, and laboratory space for expanding cells. However, compared with animal component-free medium, the use of low serum medium in clinical applications will still bring many uncertain risks [59,60]. Additionally, the hDPSCs/hTDM complexes cultured in the three media all regenerated dentin-like, pulp-like, and fibrous-like tissue, according to histomorphological analysis of our study, which indicated that ACF medium can substitute SCM for the pre-transplantation culture of hDPSCs/hTDM complexes in tissue engineering of bioengineered-root regeneration *in vivo*. Therefore, the application of ACF medium *in vitro* enhances the safety and feasibility of tissue engineering for bioengineered-root regeneration *in vivo*, promoting the clinical translation of tissue engineering in bioengineered-root regeneration.

5. Conclusion

Our work demonstrates a novel use of the animal component-free medium for culturing hDPSCs with hTDM under a 3D environment, showing that it was proved to be an alternative strategy for bioengineered-root regeneration. Clinical safety and ethical concerns associated with serum in bioengineered-root regeneration might be solved by using ACF medium for pre-transplantation culture. In our experiments, we implanted the hDPSCs/hTDM complexes subcutaneously in nude mice for *in vivo* verification. To further validate, it would be better to implant hDPSCs/hTDM complexes into the jawbone of large animals. In summary, the application of ACF medium in bioengineered-root regeneration can facilitate the transition of bioengineered-root regeneration from basic research to clinical applications.

Ethical statement

The experimental protocol was established, according to the ethical guidelines of the Helsinki Declaration and was approved by the Ethics Committee of the College of Stomatology, Chongqing Medical University (NO: 2022 (LSNo. 115)). Written informed consent was obtained from individual or guardian participants.

Availability of data and materials

All of the relevant data and materials are available from the corresponding author on reasonable request.

CRediT authorship contribution statement

Yuzhen Zhan: Writing – original draft, Investigation, Conceptualization. **Aizhuo Qian:** Writing – review & editing, Validation, Investigation. **Jieya Gao:** Visualization, Methodology. **Shiyong Ma:** Software, Methodology. **Pingmeng Deng:** Resources, Methodology. **Hefeng Yang:** Resources, Methodology. **Xiaonan Zhang:** Supervision. **Jie Li:** Writing – review & editing, Writing – original draft, Supervision, Project administration, Funding acquisition, Conceptualization.

Declaration of competing interest

The authors declare that they have no known competing financial interests or personal relationships that could have appeared to influence the work reported in this paper.

Acknowledgements

This work was supported by the National Natural Science Foundation of China [Grant No. 82071072], Open Foundation of Yunnan Key Laboratory of Stomatology, The Affiliated Stomatology Hospital of Kunming Medical University [Grant No. 2022YNKQ002], and Program for Youth Innovation in Future Medicine, Chongqing Medical University [Grant No. W0179].

Appendix A. Supplementary data

Supplementary data to this article can be found online at https://doi.org/10.1016/j.heliyon.2024.e34173.

References

[1] D.R. Burns, D.A. Beck, S.K. Nelson, A review of selected dental literature on contemporary provisional fixed prosthodontic treatment: report of the Committee on Research in Fixed Prosthodontics of the Academy of Fixed Prosthodontics, J. Prosthet. Dent 90 (5) (2003) 474–497, https://doi.org/10.1016/s0022-3913(03)00259-2.
[2] E. Abt, A.B. Carr, H.V. Worthington, Interventions for replacing missing teeth: partially absent dentition, Cochrane Database Syst. Rev. (2) (2012), https://doi.org/10.1002/14651858.CD003814.pub2.
[3] S.H. Bassir, K. El Kholy, C.Y. Chen, K.H. Lee, G. Intini, Outcome of early dental implant placement versus other dental implant placement protocols: a systematic review and meta-analysis, J. Periodontol. 90 (5) (2019) 493–506, https://doi.org/10.1002/JPER.18-0338.
[4] D.S. Koussoulakou, L.H. Margaritis, S.L. Koussoulakos, A curriculum vitae of teeth: evolution, generation, regeneration, Int. J. Biol. Sci. 5 (3) (2009) 226, https://doi.org/10.7150/ijbs.5.226.
[5] Q. Zhai, Z. Dong, W. Wang, B. Li, Y. Jin, Dental stem cell and dental tissue regeneration, Front. Med. 13 (2019) 152–159, https://doi.org/10.1007/s11684-018-0628-x.
[6] Y.D. Zhang, Z. Chen, Y.Q. Song, C. Liu, Y.P. Chen, Making a tooth: growth factors, transcription factors, and stem cells, Cell Res. 15 (5) (2005) 301–316, https://doi.org/10.1038/sj.cr.7290299.
[7] M.S. Mozaffari, G. Emami, H. Khodadadi, B. Baban, Stem cells and tooth regeneration: prospects for personalized dentistry, EPMA J. 10 (2019) 31–42, https://doi.org/10.1007/s13167-018-0156-4.
[8] Z. Gao, L. Hu, G. Liu, F. Wei, Y. Liu, Z. Liu, Z. Fan, C. Zhang, J. Wang, S. Wang, Bio-root and implant-based restoration as a tooth replacement alternative, J. Dent. Res. 95 (6) (2016) 642–649, https://doi.org/10.1177/0022034516639260.
[9] X. Yang, Y. Ma, W. Guo, B. Yang, W. Tian, Stem cells from human exfoliated deciduous teeth as an alternative cell source in bio-root regeneration, Theranostics 9 (9) (2019) 2694, https://doi.org/10.7150/thno.31801.
[10] B. Yang, G. Chen, J. Li, Q. Zou, D. Xie, Y. Chen, H. Wang, X. Zheng, J. Long, W. Tang, W. Guo, W. Tian, Tooth root regeneration using dental follicle cell sheets in combination with a dentin matrix - based scaffold, Biomaterials 33 (8) (2012) 2449–2461, https://doi.org/10.1016/j.biomaterials.2011.11.074.
[11] Y. Yuan, X. Zhang, Y. Zhan, S. Tang, P. Deng, Z. Wang, J. Li, Adipose-derived stromal/stem cells are verified to be potential seed candidates for bio-root regeneration in three-dimensional culture, Stem Cell Res. Ther. 13 (1) (2022) 234, https://doi.org/10.1186/s13287-022-02907-y.
[12] W. Guo, K. Gong, H. Shi, G. Zhu, Y. He, B. Ding, L. Wen, Y. Jin, Dental follicle cells and treated dentin matrix scaffold for tissue engineering the tooth root, Biomaterials 33 (5) (2012) 1291–1302, https://doi.org/10.1016/j.biomaterials.2011.09.068.
[13] G.T. Huang, S. Gronthos, S. Shi, Mesenchymal stem cells derived from dental tissues vs. those from other sources: their biology and role in regenerative medicine, J. Dent. Res. 88 (9) (2009) 792–806, https://doi.org/10.1177/0022034509340867.
[14] Y. Yuan, X. Zhang, Y. Zhan, S. Tang, P. Deng, Z. Wang, J. Li, Adipose-derived stromal/stem cells are verified to be potential seed candidates for bio-root regeneration in three-dimensional culture, Stem Cell Res. Ther. 13 (1) (2022) 234, https://doi.org/10.1186/s13287-022-02907-y.
[15] O. Karnieli, O.M. Friedner, J.G. Allickson, N. Zhang, S. Jung, D. Fiorentini, E. Abraham, S.S. Eaker, T.K. Yong, A. Chan, S. Griffiths, A.K. Wehn, S. Oh, O. Karnieli, A consensus introduction to serum replacements and serum-free media for cellular therapies, Cytotherapy 19 (2) (2017) 155–169, https://doi.org/10.1016/j.jcyt.2016.11.011.
[16] S. Julavijitphong, S. Wichitwiengrat, N. Tirawanchai, P. Ruangvutilert, C. Vantanasiri, T. Phermthai, A xeno-free culture method that enhances Wharton's jelly mesenchymal stromal cell culture efficiency over traditional animal serum-supplemented cultures, Cytotherapy 16 (5) (2014) 683–691, https://doi.org/10.1016/j.jcyt.2013.07.012.
[17] D.G. Halme, D.A. Kessler, FDA regulation of stem-cell-based therapies, N. Engl. J. Med. 355 (16) (2006) 1730–1735, https://doi.org/10.1056/NEJMhpr063086.
[18] M.J. Martin, A. Muotri, F. Gage, A. Varki, Human embryonic stem cells express an immunogenic nonhuman sialic acid, Nat. Med. 11 (2) (2005) 228–232, https://doi.org/10.1038/nm1181.
[19] J. van der Valk, D. Mellor, R. Brands, R. Fischer, F. Gruber, G. Gstraunthaler, L. Hellebrekers, J. Hyllner, F.H. Jonker, P. Prieto, M. Thalen, V. Baumans, The humane collection of fetal bovine serum and possibilities for serum-free cell and tissue culture, Toxicol. Vitro 18 (1) (2004) 1–12, https://doi.org/10.1016/j.tiv.2003.08.009.
[20] S. Thirumala, W.S. Goebel, E.J. Woods, Manufacturing and banking of mesenchymal stem cells, Expet Opin. Biol. Ther. 13 (5) (2013) 673–691, https://doi.org/10.1517/14712598.2013.763925.
[21] T. Burnouf, D. Strunk, M.B. Koh, K. Schallmoser, Human platelet lysate: replacing fetal bovine serum as a gold standard for human cell propagation? Biomaterials 76 (2016) 371–387, https://doi.org/10.1016/j.biomaterials.2015.10.065.
[22] L.G. Chase, S. Yang, V. Zachar, Z. Yang, U. Lakshmipathy, J. Bradford, S.E. Boucher, M.C. Vemuri, Development and characterization of a clinically compliant xeno-free culture medium in good manufacturing practice for human multipotent mesenchymal stem cells, Stem Cells Transl Med 1 (10) (2012) 750–758, https://doi.org/10.5966/sctm.2012-0072.
[23] M. Shi, Z. Zhang, R. Xu, H. Lin, J. Fu, Z. Zou, A. Zhang, J. Shi, L. Chen, S. Lv, W. He, H. Geng, L. Jin, Z. Liu, F.S. Wang, Human mesenchymal stem cell transfusion is safe and improves liver function in acute-on-chronic liver failure patients, Stem Cells Transl Med 1 (10) (2012) 725–731, https://doi.org/10.5966/sctm.2012-0034.
[24] K. Sato, T. Itoh, T. Kato, Y. Kitamura, S.C. Kaul, R. Wadhwa, F. Sato, O. Ohneda, Serum-free isolation and culture system to enhance the proliferation and bone regeneration of adipose tissue-derived mesenchymal stem cells, In Vitro Cell. Dev. Biol. Anim. 51 (5) (2015) 515–529, https://doi.org/10.1007/s11626-014-9860-0.

[25] D. Murabayashi, M. Mochizuki, Y. Tamaki, T. Nakahara, Practical methods for handling human periodontal ligament stem cells in serum-free and serum-containing culture conditions under hypoxia: implications for regenerative medicine, Hum. Cell 30 (3) (2017) 169–180, https://doi.org/10.1007/s13577-017-0161-2.
[26] C. Qu, M. Brohlin, P.J. Kingham, P. Kelk, Evaluation of growth, stemness, and angiogenic properties of dental pulp stem cells cultured in cGMP xeno-/serum-free medium, Cell Tissue Res. 380 (1) (2020) 93–105, https://doi.org/10.1007/s00441-019-03160-1.
[27] Y. Kawase-Koga, Y. Fujii, D. Yamakawa, M. Sato, D. Chikazu, Identification of neurospheres generated from human dental pulp stem cells in xeno-/serum-free conditions, Regen Ther 14 (2020) 128–135, https://doi.org/10.1016/j.reth.2019.11.006.
[28] L. Xiao, T. Tsutsui, Characterization of human dental pulp cells-derived spheroids in serum-free medium: stem cells in the core, J. Cell. Biochem. 114 (11) (2013) 2624–2636, https://doi.org/10.1002/jcb.24610.
[29] S.Y. Lee, G.W. Huang, J.N. Shiung, Y.H. Huang, J.H. Jeng, T.F. Kuo, J.C. Yang, W.C. Yang, Magnetic cryopreservation for dental pulp stem cells, Cells Tissues Organs 196 (1) (2012) 23–33, https://doi.org/10.1159/000331247.
[30] M. Mochizuki, T. Nakahara, Establishment of xenogeneic serum-free culture methods for handling human dental pulp stem cells using clinically oriented in-vitro and in-vivo conditions, Stem Cell Res. Ther. 9 (1) (2018) 25, https://doi.org/10.1186/s13287-017-0761-5.
[31] R. Li, W. Guo, B. Yang, L. Guo, L. Sheng, G. Chen, Y. Li, Q. Zou, D. Xie, X. An, Y. Chen, W. Tian, Human treated dentin matrix as a natural scaffold for complete human dentin tissue regeneration, Biomaterials 32 (20) (2011) 4525–4538, https://doi.org/10.1016/j.biomaterials.2011.03.008.
[32] L. Guo, J. Li, X. Qiao, M. Yu, W. Tang, H. Wang, W. Guo, W. Tian, Comparison of odontogenic differentiation of human dental follicle cells and human dental papilla cells, PLoS One 8 (4) (2013) e62332, https://doi.org/10.1371/journal.pone.0062332.
[33] A.J. Lomakin, K.C. Lee, S.J. Han, D.A. Bui, M. Davidson, A. Mogilner, G. Danuser, Competition for actin between two distinct F-actin networks defines a bistable switch for cell polarization, Nat. Cell Biol. 17 (11) (2015) 1435–1445, https://doi.org/10.1038/ncb3246.
[34] A. Elosegui-Artola, A. Jorge-Penas, O. Moreno-Arotzena, A. Oregi, M. Lasa, J.M. Garcia-Aznar, E.M. De Juan-Pardo, R. Aldabe, Image analysis for the quantitative comparison of stress fibers and focal adhesions, PLoS One 9 (9) (2014) e107393, https://doi.org/10.1371/journal.pone.0107393.
[35] J.R.K. Samal, V.K. Rangasami, S. Samanta, O.P. Varghese, O.P. Oommen, Discrepancies on the role of oxygen gradient and culture condition on mesenchymal stem cell fate, Adv Healthc Mater 10 (6) (2021) e2002058, https://doi.org/10.1002/adhm.202002058.
[36] L.A. Costa, N. Eiro, M. Fraile, L.O. Gonzalez, J. Saa, P. Garcia-Portabella, B. Vega, J. Schneider, F.J. Vizoso, Functional heterogeneity of mesenchymal stem cells from natural niches to culture conditions: implications for further clinical uses, Cell. Mol. Life Sci. 78 (2) (2021) 447–467, https://doi.org/10.1007/s00018-020-03600-0.
[37] D. Brunner, J. Frank, H. Appl, H. Schoffl, W. Pfaller, G. Gstraunthaler, Serum-free cell culture: the serum-free media interactive online database, ALTEX 27 (1) (2010) 53–62, https://doi.org/10.14573/altex.2010.1.53.
[38] K. Zhang, L. Yu, F.R. Li, X. Li, Z. Wang, X. Zou, C. Zhang, K. Lv, B. Zhou, S. Mitragotri, M. Chen, Topical application of exosomes derived from human umbilical cord mesenchymal stem cells in combination with sponge spicules for treatment of photoaging, Int J Nanomedicine 15 (2020) 2859–2872, https://doi.org/10.2147/IJN.S249751.
[39] Z.D. Shi, J. Tchao, L. Wu, A.J. Carman, Precision installation of a highly efficient suicide gene safety switch in human induced pluripotent stem cells, Stem Cells Transl Med 9 (11) (2020) 1378–1388, https://doi.org/10.1002/sctm.20-0007.
[40] A. Caye, K. Rouault-Pierre, M. Strullu, E. Lainey, A. Abarrategi, O. Fenneteau, C. Arfeuille, J. Osman, B. Cassinat, S. Pereira, F. Anjos-Afonso, E. Currie, L. Ariza-McNaughton, V. Barlogis, J.H. Dalle, A. Baruchel, C. Chomienne, H. Cave, D. Bonnet, Despite mutation acquisition in hematopoietic stem cells, JMML-propagating cells are not always restricted to this compartment, Leukemia 34 (6) (2020) 1658–1668, https://doi.org/10.1038/s41375-019-0662-y.
[41] H. Wang, D. Li, Z. Zhai, X. Zhang, W. Huang, X. Chen, L. Huang, H. Liu, J. Sun, Z. Zou, Y. Fan, Q. Ke, X. Lai, T. Wang, X. Li, H. Shen, A.P. Xiang, W. Li, Characterization and therapeutic application of mesenchymal stem cells with neuromesodermal origin from human pluripotent stem cells, Theranostics 9 (6) (2019) 1683–1697, https://doi.org/10.7150/thno.30487.
[42] N. Paiboon, W. Kamprom, S. Manochantr, C. Tantrawatpan, D. Tantikanlayaporn, S. Roytrakul, P. Kheolamai, Gestational tissue-derived human mesenchymal stem cells use distinct combinations of bioactive molecules to suppress the proliferation of human hepatoblastoma and colorectal cancer cells, Stem Cell. Int. 2019 (2019) 9748795, https://doi.org/10.1155/2019/9748795.
[43] X. Gao, Y. Wu, L. Liao, W. Tian, Oral organoids: progress and challenges, J. Dent. Res. 100 (5) (2021) 454–463, https://doi.org/10.1177/0022034520983808.
[44] X. Yang, Y. Ma, W. Guo, B. Yang, W. Tian, Stem cells from human exfoliated deciduous teeth as an alternative cell source in bio-root regeneration, Theranostics 9 (9) (2019) 2694–2711, https://doi.org/10.7150/thno.31801.
[45] G. Chen, J. Chen, B. Yang, L. Li, X. Luo, X. Zhang, L. Feng, Z. Jiang, M. Yu, W. Guo, W. Tian, Combination of aligned PLGA/Gelatin electrospun sheets, native dental pulp extracellular matrix and treated dentin matrix as substrates for tooth root regeneration, Biomaterials 52 (2015) 56–70, https://doi.org/10.1016/j.biomaterials.2015.02.011.
[46] H. Li, J. Sun, J. Li, H. Yang, X. Luo, J. Chen, L. Xie, F. Huo, T. Zhu, W. Guo, W. Tian, Xenogeneic bio-root prompts the constructive process characterized by macrophage phenotype polarization in rodents and nonhuman primates, Adv Healthc Mater 6 (5) (2017), https://doi.org/10.1002/adhm.201601112.
[47] S. Zhang, Y. Yang, S. Jia, H. Chen, Y. Duan, X. Li, S. Wang, T. Wang, Y. Lyu, G. Chen, W. Tian, Exosome-like vesicles derived from Hertwig's epithelial root sheath cells promote the regeneration of dentin-pulp tissue, Theranostics 10 (13) (2020) 5914–5931, https://doi.org/10.7150/thno.43156.
[48] J. Xiao, D. Yang, Q. Li, W. Tian, W. Guo, The establishment of a chemically defined serum-free culture system for human dental pulp stem cells, Stem Cell Res. Ther. 9 (1) (2018) 191, https://doi.org/10.1186/s13287-018-0928-8.
[49] X. Yao, R. Peng, J. Ding, Effects of aspect ratios of stem cells on lineage commitments with and without induction media, Biomaterials 34 (4) (2013) 930–939, https://doi.org/10.1016/j.biomaterials.2012.10.052.
[50] R. Peng, X. Yao, J. Ding, Effect of cell anisotropy on differentiation of stem cells on micropatterned surfaces through the controlled single cell adhesion, Biomaterials 32 (32) (2011) 8048–8057, https://doi.org/10.1016/j.biomaterials.2011.07.035.
[51] H. Wolfenson, B. Yang, M.P. Sheetz, Steps in mechanotransduction pathways that control cell morphology, Annu. Rev. Physiol. 81 (2019) 585–605.
[52] S. Dalton, Linking the cell cycle to cell fate decisions, Trends Cell Biol. 25 (10) (2015) 592–600, https://doi.org/10.1016/j.tcb.2015.07.007.
[53] J. Sabbagh, M. Ghassibe-Sabbagh, M. Fayyad-Kazan, F. Al-Nemer, J.C. Fahed, A. Berberi, B. Badran, Differences in osteogenic and odontogenic differentiation potential of DPSCs and SHED, J. Dent. 101 (2020) 103413, https://doi.org/10.1016/j.jdent.2020.103413.
[54] L. Ye, M. MacDougall, S. Zhang, Y. Xie, J. Zhang, Z. Li, Y. Lu, Y. Mishina, J.Q. Feng, Deletion of dentin matrix protein-1 leads to a partial failure of maturation of predentin into dentin, hypomineralization, and expanded cavities of pulp and root canal during postnatal tooth development, J. Biol. Chem. 279 (18) (2004) 19141–19148, https://doi.org/10.1074/jbc.M400490200.
[55] T. Sreenath, T. Thyagarajan, B. Hall, G. Longenecker, R. D'Souza, S. Hong, J.T. Wright, M. MacDougall, J. Sauk, A.B. Kulkarni, Dentin sialophosphoprotein knockout mouse teeth display widened predentin zone and develop defective dentin mineralization similar to human dentinogenesis imperfecta type III, J. Biol. Chem. 278 (27) (2003) 24874–24880, https://doi.org/10.1074/jbc.M303908200.
[56] D. Kajdaniuk, B. Marek, H. Borgiel-Marek, B. Kos-Kudla, Transforming growth factor beta1 (TGFbeta1) in physiology and pathology, Endokrynol. Pol. 64 (5) (2013) 384–396, https://doi.org/10.5603/EP.2013.0022.
[57] J. Du, M. Li, Functions of Periostin in dental tissues and its role in periodontal tissues' regeneration, Cell. Mol. Life Sci. 74 (2017) 4279–4286.
[58] M. Kanafi, D. Majumdar, R. Bhonde, P. Gupta, I. Datta, Midbrain cues dictate differentiation of human dental pulp stem cells towards functional dopaminergic neurons, J. Cell. Physiol. 229 (10) (2014) 1369–1377, https://doi.org/10.1002/jcp.24570.
[59] A. Parker, H. Shang, M. Khurgel, A. Katz, Low serum and serum-free culture of multipotential human adipose stem cells, Cytotherapy 9 (7) (2007) 637–646, https://doi.org/10.1080/14653240701508452.
[60] D. Li, Q. Zhong, T. Liu, J. Wang, Cell growth stimulating effect of Ganoderma lucidum spores and their potential application for Chinese hamster ovary K1 cell cultivation, Bioproc. Biosyst. Eng. 39 (6) (2016) 925–935, https://doi.org/10.1007/s00449-016-1572-2.